PERGAMON

International Journal of Heat and Mass Transfer 44 (2001) 1913–1924

International Journal of HEAT and MASS TRANSFER

www.elsevier.com/locate/ijhmt

The density field of coaxial jets with large velocity ratio and large density differences

M. Favre-Marinet *, E.B. Camano Schettini [1]

INPG, UJF, CNRS, Laboratoire des Ecoulements Géophysiques et Industriels, Institut de Mécanique de Grenoble B.P. 53X, 38041 Grenoble Cedex, France

Received 17 June 1999; received in revised form 10 July 2000

Abstract

This paper describes an experimental investigation of the density field of coaxial jets with large density differences. These flows are characterised by a low velocity–high density inner jet surrounded by a high velocity–low density annular jet. The density field was determined by a thermo-anemometric method based on a new version of an aspirating probe. Measurements show that mixing is directly dependent upon the flow dynamics in the near-field region. As a result, density effects on mixing as well as on the flow dynamics are rather well taken into account by considering the specific outer to inner jet momentum flux ratio M and not separately the density and the velocity ratios. For a given value of M, however, a slight enhancement of mixing is found for density ratios much smaller than one ($\approx$0.14).

Keywords: Coaxial jets; Large density differences; Hot wire anemometry; Density measurements; Mixing; Transition to Turbulence

1. Aim of research

Coaxial jets have been investigated to a great extent, because they are present in several practical applications, especially in the propulsion and combustion areas. Most studies have considered isothermal homogeneous coaxial jets. For example, Champagne and Wygnanski [1] determined the mean and turbulent velocity fields of isothermal air–air coaxial jets with a ratio of outer to inner velocity r_v ranging from 0.5 to 10. In a series of papers, Ko and co-workers identified coherent structures in the near-field of coaxial jets and investigated their properties, both for values of r_v lower than one [2–4] and for r_v higher than one [5,6]. In a visualisation study, Dahm et al. [7] analysed the various vortex patterns and their interaction dynamics for a large range of r_v-values (0.59–4.16). All these studies were restricted to rather moderate values of r_v and no recirculation was found in the central region of the corresponding coaxial jets. However, it is obvious that a strong recirculation takes place near the nozzle in annular jets ($r_v = \infty$) [8] and there is an upper limit of r_v beyond which recirculation occurs. Recently, coaxial jets with large velocity ratio have been extensively investigated in our laboratory and the conditions for onset of recirculation have been determined [9–11]. In relation to this problem, the velocity and pressure fields were analysed by Chigier et al. [12] in the near-region of concentric jets separated by a large interface. Moreover, these authors performed concentration measurements on the jet-axis for r_v varying between 0 and 9.72 by using CO_2 as a tracer gas in the annular-jet and by heating the central jet. However, it must be pointed out that temperature and concentration may be considered as passive contaminants in these latter experiments.

In fact, very few investigations have considered the effects of density on coaxial jets although large density differences may be present in industrial processes. Gladnick et al. [13] found an increase in mixing with increasing velocity ratio (limited to two in their study) in

* Corresponding author. Tel.: +33-4-7682-5049; fax: +33-4-7682-5271.

E-mail address: favre@hmg.inpg.fr (M. Favre-Marinet).

[1] Present address: Instituto de Pesquisas Hidraulicas, Universidade Federal de Rio Grande do, Sul, CP 15029, 91501-970 Porto Alegre, Brazil.

0017-9310/01/$ - see front matter
PII: S0017-9310(00)00240-4

Nomenclature

D	nozzle diameter
E	aspirating probe response
Fr	Froude number
L	potential core length
L_p	potential core length as defined from the density field
M	outer to inner specific momentum flux ratio
M_c	critical value of M corresponding to onset of recirculation
r	distance to jet-axis
r_v	outer to inner bulk velocity ratio
Re_M	Reynolds number defined in Table 2
S	outer to inner density ratio
U	jet exit mean velocity
x	distance to nozzle
X	mole fraction

Greek symbols

β	diameter ratio
δ	mixing layer width
ξ	length of the inertia-dominated region
ρ	density
ρ^*	normalised density $= (\rho-\rho_e)/(\rho_i-\rho_e)$ (Eq. (1)) or $(\rho-\rho_{He})/(\rho_\infty-\rho_{He})$ (Eq. (2))
$\overline{\rho^*}$	mean density
$\rho^{*\prime}$	density fluctuations RMS

Notations

$(\,)_i$	relative to inner jet
$(\,)_e$	relative to external jet
$(\,)_\infty$	relative to ambient fluid

an axisymmetric jet flow of CFC-12 issuing into a coannular jet flow of air (outer to inner density ratio S:0.26). This was attributed to the presence of annular vortex rings originating in the mixing layer between the inner jet and coannular flow.

The present research aims at simulating the flow conditions of liquid propellant rocket engine injectors which are characterised by a low velocity–high density inner jet surrounded by a high velocity–low density coannular jet. By using various gas combinations (air, helium, SF_6), it is possible to reach very large density differences in the flow field near the nozzle. Two-phase flows aspects are not considered in the present study. In a previous paper [14], we have shown that density effects on the jets dynamics are well taken into account by considering the specific outer to inner jet momentum flux ratio M and not separately the density and velocity ratios. In particular, the critical condition for incepient recirculation was found to be $M \approx 50$, both for air/air and helium/air jets, although the parameter S varied by a factor 7 in the two cases.

The present paper is concerned with the effects of large density differences on mixing in coaxial jets. The density field was determined by using thermo-anemometry and analysed in relation to the flow dynamics. In particular, the present work addresses the issue of the parameters which control the mixing process in these coaxial jets.

2. Experimental arrangement and instrumentation

2.1. Experimental set-up

The experimental set-up (Fig. 1) consists of a pair of concentric axisymmetric nozzles discharging into quiescent ambient air. The inner nozzle is supplied by air

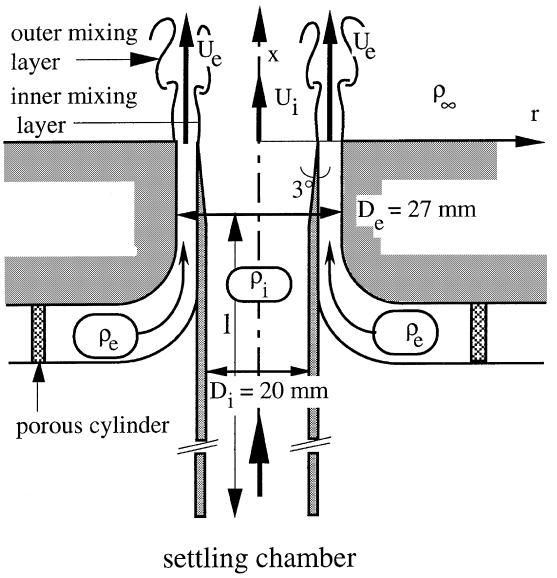

Fig. 1. Sketch of the coaxial jet.

or SF_6 from a settling chamber followed by a tube 135 mm long (contraction ratio:14). The final part of the central nozzle is slightly diverging (3°) so as to reduce the splitter wall thickness (0.2 mm) and to minimize the corresponding wake effects. The annular nozzle is supplied by air or helium. The flow enters the outer nozzle radially through an annular porous cylinder (radius 38 mm) and is deviated downstream in the axial direction.

2.2. Flow conditions

The experimental conditions are given in Table 1. The non-dimensional governing parameters are as shown in Table 2. The Reynolds number Re_M is based on

Table 1
Experimental conditions

	Diameter (mm)	Bulk velocity	Density
Inner jet (i)	$D_i = 20$	U_i	ρ_i
Outer jet (e)	$D_e = 27$	U_e	ρ_e
Ambient fluid			ρ_∞

a hypothetical jet with external fluid properties and a velocity such as to have the same total momentum flux. It is proportional to the external Reynolds number: $Re_{ext} = \rho_e U_e D_e/\mu_e$. For pure helium/air jets ($U_e = 16$ m/s), typical values are:

$$Re_{ext} = 3200, \quad 2100 < Re_M < 2400$$

The velocity ratio r_v was varied by changing the inner velocity (inner Reynolds number $Re_i = \rho_i U_i D_i/\mu_i$) and by keeping the outer velocity constant (16 m/s for helium). The flow rates were controlled by sets of sonic throat orifices of different sizes placed upstream of the settling chambers. In most experiments, the jet issued into ambient air. To test the effect of ambient fluid density, some measurements were performed with the jet issuing into a chamber filled with helium (cross-section 0.66 m × 0.90 m). For practical reasons, the experiments were conducted with one nozzle geometry only and effects of diameter ratio were not investigated. Details about flow conditions may be found in [14]. The flow is laminar at the jet exit. The inner jet velocity profile corresponds to a central flow of uniform velocity surrounded by developing laminar boundary layers.

The density was normalised with the values at the exit plane (in most cases, $\rho_\infty = \rho_i$):

$$\rho^* = (\rho - \rho_e)/(\rho_i - \rho_e) \tag{1}$$

so that the non-dimensional density varies within the interval (0–1). It may be easily shown that ρ^* is equal to the ratio, $(X - X_e)/(X_i - X_e)$, where X stands for the mole fraction of one component in the mixture.

For the few experiments conducted with round jets ($U_e = 0$) or annular jets ($U_i = 0$) of helium issuing into the ambient air (Section 3), the definition of ρ^* was modified and was given by:

$$\rho^* = (\rho - \rho_{He})/(\rho_\infty - \rho_{He}), \tag{2}$$

where ρ_{He} is the density of helium at the ambient temperature. The density RMS fluctuations ($\sqrt{\overline{\rho^{*\prime 2}}}$) was denoted $\rho^{*\prime}$.

2.3. Instrumentation

Density measurements were performed with a new design of the aspirating probe, first developed by Zawacki and Weinstein [15] and used by Brown and Rebollo [16] in the investigation of inhomogeneous mixing layers, then later on by several researchers. It consists of a very thin tube connected to a vacuum pump. In previous versions of the probe, a hot-wire was placed inside the tube and was exposed to a gas mixture extracted from the measurement point. In the original version, the probe was designed with a contracted area. When the aspirating pressure is lower than a critical value, the suction flow rate is blocked at a constant value for a mixture of given composition and for constant upstream stagnation conditions. The hot-wire is then only sensitive to density but insensitive to velocity. Such a probe was used by Ahmed and So in a swirling flow [17], where the stagnation pressure varies radially. In these unfavourable conditions, the authors have found that the response errors due to the variable stagnation pressure are negligible. This result will probably also hold in jets, where pressure variations are small. We have tried various arrangements of the probe with the aim of investigating different types of flows. In a first version designed for a boundary layer study, the front of the probe consisted of a cylindrical tube 25 mm in length in order to reduce interference effects of the probe body on the near-wall flow. It has been observed that this arrangement leads to a rather large time-response when the hot-wire is placed inside the probe body downstream from the front tube. For example, tests in a shock-tube [18] revealed a time-response of 20 ms for a probe equipped with an hypodermic needle (I.D. 360 μm, O.D. 700 μm, length 25 mm). An improvement of the time-response of the probe was achieved by placing the hot-wire at the entrance of the suction tube which was chosen as small as possible (I.D. 100 μm, O.D. 300 μm, Fig. 2, [19]). This arrangement avoids bias effects due to mass transfer and mixing inside the tube. The hot-wire was 4 μm in diameter and was overheated at a ratio 0.5. Hot-wire measurements were made with AALAB-SYSTEMS

Table 2
Non-dimensional parameters

Diameter ratio	$\beta = D_e/D_i$	1.35
Bulk velocity ratio	$r_v = U_e/U_i$	$3 < r_v < 70$
Density ratio	$S = \rho_e/\rho_i$	$0.028 < S < 1$
Specific momentum flux ratio	$M = r_v^2 S$	$1 < M < 200$
External Reynolds number	$Re_{ext} = \rho_e U_e D_e/\mu_e$	
Reynolds number	$Re_M = Re_{ext}[1 + (1 - M)/\beta^2 M]^{1/2}$	

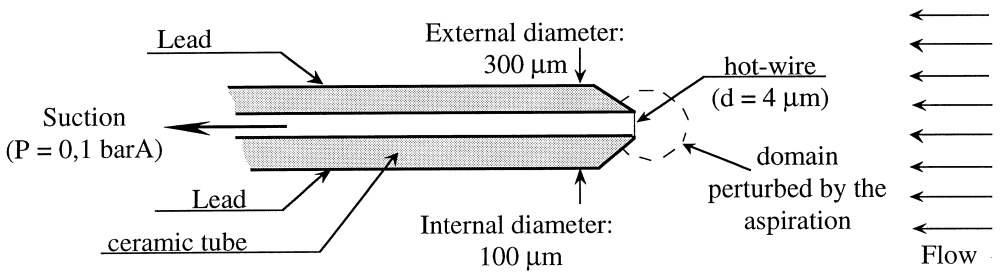

Fig. 2. Sketch of the aspirating probe.

anemometers. Data acquisition and processing were performed via a 15 bit analogic-digital converter IOtech 488/16 connected to a Macintosh IIci computer.

2.4. Accuracy and resolution

The probe was calibrated in the exit-plane of the inner nozzle flow with known velocity and density. Calibration maps (Fig. 3) show that the probe response E is quite insensitive to velocity in a very large range of flow conditions. Fig. 3 shows, however, small departures from horizontal lines for velocities less than 1 m/s and for high concentrations of helium. These errors can be probably attributed to local variations of density. At these low jet velocities, ambient air patches driven by gravity forces can probably penetrate the nozzle which is in the upward direction and contaminate the jet flow. It has been verified that the observed deviations in E from a constant value can be completely avoided by placing the probe a little upstream from the jet nozzle exit-plane.

The working principle of the probe requires a significant local perturbation of the flow since nearly sonic conditions are maintained at the tube entrance. Consequently, the upstream flow is perturbed near the entrance of the tube over a distance of the order of 1. Fortunately, the perturbation velocity which is due to the effect of suction decreases very rapidly with r, the distance to the probe (roughly as $1/r^2$). The length scale l was estimated to be of the order of 1 mm in unfavourable conditions (low velocities $\approx$2 m/s) from a computation based on potential flow theory and also from measurements in a thin mixing layer [19]. The time-response τ of the probe corresponds to the transit time of a fluid parcel on the distance l. The same computation gives $\tau \approx 1$ ms. These probe characteristics have been checked in a helium–air mixing layer and in the far-field of a helium–air jet. The dynamic behaviour of the probe has been tested in a very thin wake behind a splitter plate separating two flows of equal velocities (8.5 m/s) and different densities (air/helium). Fig. 4 shows that the spectra given by the aspirating probe and a hot-wire are very similar, even at frequencies as high as 1000 Hz (note that the hot-wire spectra have been shifted by one decade for a sake of clarity). Moreover, in the first

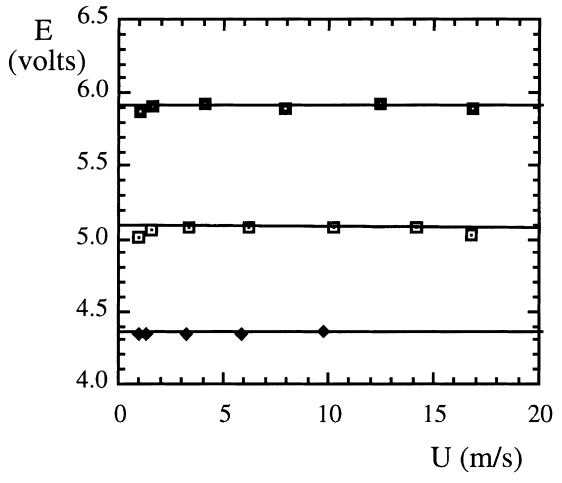

Fig. 3. Aspirating probe calibration data: (■) $S = 0.138$; (□) $S = 0.655$; (◆) $S = 1$.

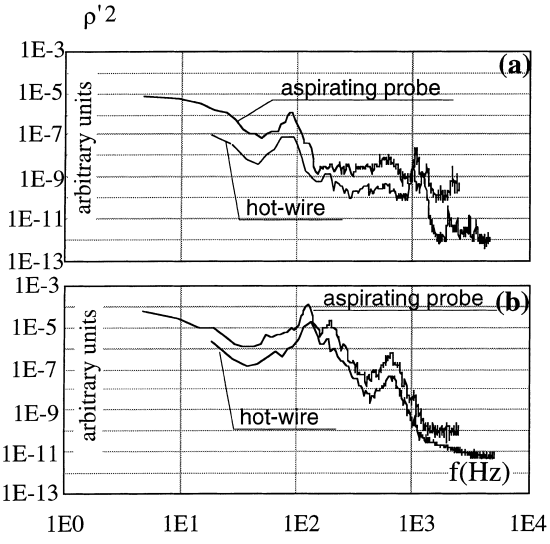

Fig. 4. Spectra in a variable density wake. Comparison of aspirating probe hot-wire responses. (a) $x = 1$ mm, (b) $x = 20$ mm.

twenty diameters of a helium–air jet, the measured mean density and the corresponding RMS fluctuation are in rather good agreement with the results of Pitts [20]. The inverse of the mean mole fraction of helium, X_{He}, increases along a straight line on the jet-axis with a slope K_0 when the distance to the nozzle is normalised by the effective diameter D_{eff} $(= D_i(\rho_i/\rho_\infty)^{1/2})$, according to:

$$\frac{1}{X_{He}} = K_0 \frac{x - x_0}{D_{eff}}. \tag{3}$$

The value of 0.24 found for K_0 is 20% higher than that deduced from Pitts measurements (see [19] for further details). This discrepancy may be attributed to the absence of co-flow in the present experiments and perhaps to slight buoyancy effects as discussed hereafter.

3. Buoyancy effects

In variable density flows, it is important to address the issue of gravity effects and to clearly identify whether the variations of density give rise to buoyancy effects or play a major role by themselves. From a fundamental point of view, buoyancy effects are characterised by the non-dimensional Froude number Fr_i expressing the ratio of the forces of inertia and gravity. For a round jet of diameter D_i, initial velocity U_i and density ρ_i issuing into the ambient fluid of density ρ_∞, the Froude number may be defined by:

$$Fr_i = U_i^2/g \frac{\rho_\infty - \rho_i}{\rho_i} D_i. \tag{4}$$

According to Chen and Rodi [21], the jet is dominated by inertia up to the distance ξ to the nozzle defined by:

$$\xi = 0.5 D_i Fr_i^{1/2} S^{1/4}. \tag{5}$$

For coaxial jets with density differences, the Froude number is not so easily defined. The main difficulty is to define the characteristic length scale of the buoyancy forces. If we consider the extreme case of an annular jet of outer diameter D_e, initial velocity U_e and density ρ_e, then the central region is dominated by an intense recirculation in the first jet diameter. In our experiment, the extent of this bubble of recirculation ($\approx 0.8 D_e$ [14]) is such that mixing with the external ambient fluid does not influence the central part of the annular jet. As a result, the recirculation region is roughly homogeneous at the density ρ_e. It seems therefore appropriate to characterize the buoyancy forces by the outer diameter of the jet D_e. In this case, the Froude number may be defined by:

$$Fr_e = U_e^2/g \frac{\rho_\infty - \rho_e}{\rho_e} D_e. \tag{6}$$

In the present study, the flow dynamics are dominated by the outer jet development since the velocity ratio r_v is much larger than one, especially for helium/air jets. Consequently, it seems reasonable to extend the definition of the Froude number as given by Eq. (6) to these jets.

Most present experiments on helium/air jets were conducted with $U_e = 16$ m/s, which leads to $Fr_e = 217$. If the result on round jet is applied to coaxial jets in substituting subscript $(\,)_i$ by $(\,)_e$ in Eq. (5), we find that the inertia-dominated region extends up to 4.5 D_e. Since we are interested in the near-field region of coaxial jets, it is concluded that buoyancy effects are likely to play a minor role on mixing in this region.

This conclusion is further supported by experiments carried out in helium–air jets with the two nozzles having opposite directions (up/down, Fig. 5(a)). Fig. 5(b) shows the centreline distribution of the mean density when only the central nozzle is fed with helium (axisymmetric jet). For this arrangement, ρ^* increases from 0 at the nozzle to 1 in the far-field of the jet according to Eq. (2). The curves obtained with the two opposite directions of gravity relative to the jet begin to separate at $6D_i$. This is a little more than the result ($4D_i$) as given by Eq. (5). When the nozzle is directed downward (gravity-opposed flow), buoyancy forces become dominant beyond $15D_i$ and the flow cannot penetrate the ambient fluid farther than $20D_i$. In this case, low-density fluid from the far region (≈ 15–$20D_i$) moves upward in the neighbourhood of the jet and is then entrained across the jet interface instead of the surrounding air. This explains why the mean density is lower in the gravity-opposed case than in the gravity-aided one in the interval ($6D_i$–$15D_i$).

The same trends are found for annular jets (Fig. 5(c)). However, the inertia-dominated region is a little larger ($8D_i$) than for round jets. This result is again a little higher than that predicted by Eqs. (5) and (6) ($6D_i$). In the gravity-aided case, the mean concentration departs from 0 very close to the nozzle, contrary to the other case. The main interest of the study being the mixing in coaxial jets, no further experiments were carried out to explore the near-field of the annular jets and the striking behaviour of the gravity-aided annular jet remains so far unexplained.

Finally, Fig. 5(d) shows the mean density evolution for a coaxial jet defined by $r_v = 8$ $(M = 9)$. The results corresponding to the two opposite directions of gravity relative to the jet are the same up to $8D_i$. The curve obtained with helium as the ambient fluid will be discussed later.

These results are in rather good agreement with the predictions as given by Eqs. (5) and (6) and demonstrate that buoyancy effects are negligible in the near-field region ($\approx 8D_i$) of coaxial jets with high velocity ratio in the conditions considered in this study.

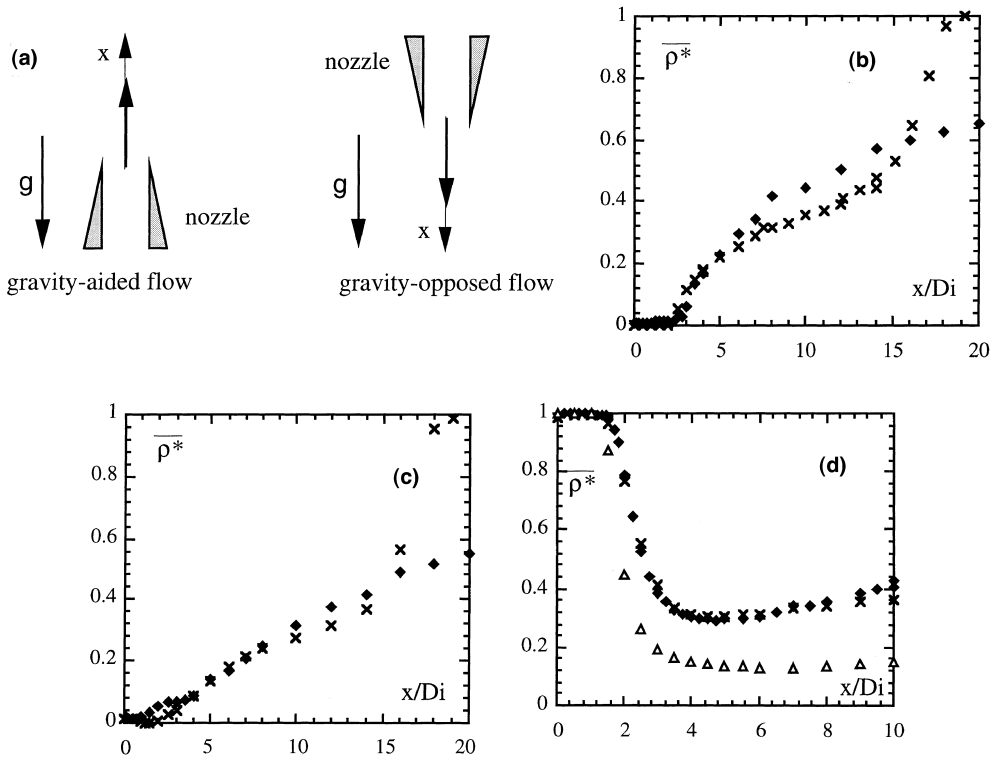

Fig. 5. Centreline variations of mean density for helium/air jets with the two nozzles having opposite directions: (◆) gravity-aided flow; (×) gravity-opposed flow: (a) sketch of the facility; (b) round jets; (c) annular jets; (d) $r_v = 8$ (△) helium as ambient fluid.

4. Results

Before describing the density field characteristics, it is worth recalling the main features found for these coaxial jets with large velocity ratio [14]. It was shown that a regime of recirculation occurs for M higher than a critical value ($M_c \approx 50$). The mean positions of the recirculation bubble on the jet-axis were determined by various methods (LDA, thermo-anemometry, visualisations). Its downstream end slightly depends on M. It moves from 1.3 D_i for incipient recirculation to about 1 D_i for an annular jet. On the other hand, the upstream end of the recirculation bubble continuously moves upstream when M is increased. Visualisations showed that this upstream end strongly fluctuates at low-frequency.

Most measurements which are presented thereafter were obtained in coaxial helium–air jets flowing in the vertical upward direction. For this combination of gas, it has been verified that the results obtained in the near-field are not affected by viscous effects. This point was checked by comparing density measurements for $Re_M = 2520$ and 1260 in pure helium/air jets with $r_v = 8$ (not shown here). It was found that the centreline variations both for $\overline{\rho^*}$ and $\rho^{*\prime}$ match closely for the two values of Re_M in the region of interest (up to $20D_i$). Density effects were tested by comparing coaxial jets with strong density differences (pure helium–pure air jets; $S = 0.138, U_e = 16$ m/s) to coaxial jets with a moderate value of S ($S = 0.655$) obtained by using a air–helium mixture as the annular jet fluid. In this latter case, the external velocity ($U_e = 7.3$ m/s) was determined in order to give the same external momentum flux as in the former one. The corresponding value of S was chosen in order to measure density differences with reasonable accuracy. Although S is not very close from one, it is thought that density effects are contrasted by a comparison between the two situations since the relative initial density differences are 2.5 times stronger in the first case ($(\rho_i - \rho_e)/\rho_i = 0.86$) than in the second one (0.35).

4.1. Density measurements along the jet axis

4.1.1. Influence of velocity and density ratios on mixing

Fig. 6 compares the normalised mean and RMS density distributions along the jet-axis for two experiments conducted with the same value of the velocity ratio r_v. The results are dramatically different and obviously demonstrate a significant effect of S on the density field when r_v is kept constant. The potential core length L_p is considerably reduced by an increase of S,

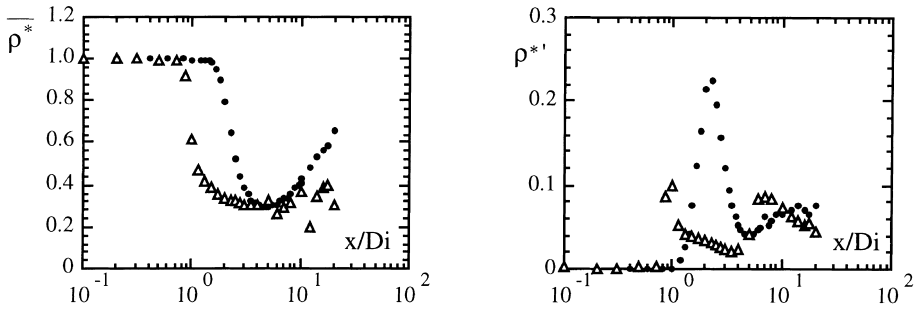

Fig. 6. Centreline variations of density for a fixed value of the velocity ratio $r_v = 8$; left: mean value, right: RMS fluctuations; (△) $S = 0.655$, $M = 42$, (●) $S = 0.138$, $M = 9$.

indicating an enhancement of mixing for a given value of r_v. In fact, Fig. 6 shows that L_p is twice as short for $S = 0.655$ as for $S = 0.138$ for $r_v = 8$. On the contrary, mixing is much less affected by S, when the specific momentum flux ratio M is kept constant (Fig. 7). The two values of M which have been chosen for illustrating this point correspond to coaxial jets without recirculation ($M = 9$) or with strong recirculation ($M = 144$). It is observed that for $S = 0.655$ the minimum of $\overline{\rho^*}$ is a little higher than for $S = 0.138$. However, the overall distributions of $\overline{\rho^*}$ and $\rho^{*\prime}$ are very similar for the two values of S. These results also hold for the regime of

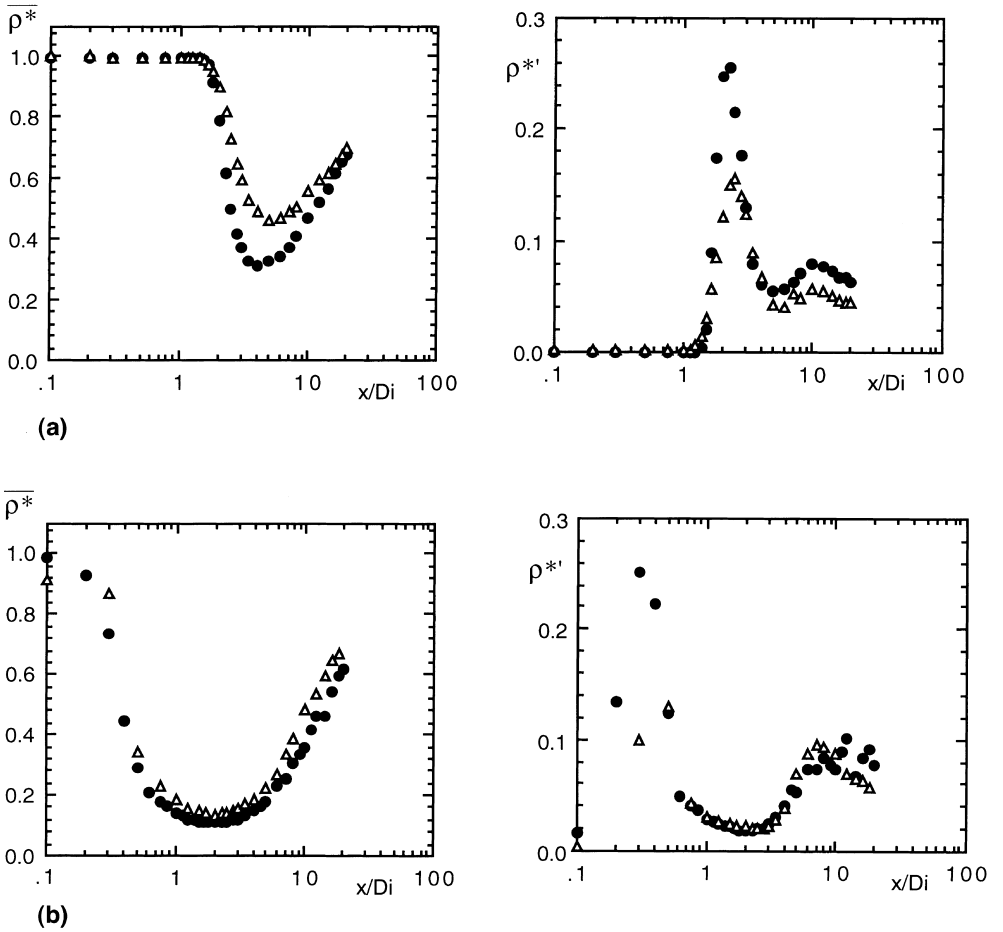

Fig. 7. Centreline variations of density for fixed values of the specific momentum ratio M: (a) $M = 9$; (b) $M = 144$ left: mean value, right: RMS fluctuations; (△) $S = 0.655$, (●) $S = 0.138$.

recirculation ($M = 144$). It may therefore be concluded that effects of large density differences on mixing in coaxial jets are rather well taken into account by considering the specific momentum ratio M instead of the velocity and density ratios separately. The same conclusion was also drawn about the jet development [14].

4.1.2. Influence of specific momentum ratio on mixing

The centreline distributions of the mean and RMS fluctuation density are strongly affected by M (Fig. 8). The curves relative to $\rho^{*\prime}$ have been separated in two parts for sake of clarity. $\overline{\rho^*}$ starts decreasing (Fig. 8(a)) and $\rho^{*\prime}$ starts rising (Figs. 8(b) and (c)) when the inner mixing layers merge on the jet-axis. The corresponding length of the potential core L_ρ decreases with increasing M. Very intense fluctuations take place in the near-field region and $\rho^{*\prime}$ reaches a maximum value on the jet-axis downstream from the end of the potential core. These density fluctuations are most probably related to the crossing of large scale structures near the end of the potential core ($M < M_c$) or to large oscillations of the upstream recirculation bubble boundary for the highest values of M ($M > M_c$), as shown by visualisations [14]. The low minimum values of the mean density ($\overline{\rho^*}_{min}$) and of $\rho^{*\prime}$ downstream from the recirculation bubble (for $M > 50$) correspond to a high degree of mixing in the initial inner region. For lower values of M (< 50), the mean density minimum on the jet-axis occurs further downstream and, at this distance, $\overline{\rho^*}$ is significantly affected by mixing with outer ambient air. It follows that $\overline{\rho^*}_{min}$ increases substantially with decreasing M. It is worth noting that all the $\overline{\rho^*}$ axial profiles for given values of M collapse on a single curve for sufficiently high values of x/D_i. As a final remark, it is clear from these results that the presence of recirculation does not affect dramatically the global features of the $\overline{\rho^*}$ and $\rho^{*\prime}$ distributions, and cannot therefore be deduced from such measurements of density.

4.2. Cross-sectional profiles

Fig. 9 compares mean and RMS fluctuations density profiles across the jet for strong and moderate density ratios and for the same value of M ($M = 9$). Note that the scale of abscissa has been magnified three-fold for the farthest profiles ($x/D_i \geqslant 3.5$) in comparison to the nearest ones. Since the global features are very similar for the two sets of measurements, these results clearly confirm that the change in density is satisfactorily taken into account by grouping r_v and S in the specific flux momentum ratio M.

The mixing process gives rise to shear layer growth on the inner and outer sides of the annular jet. As a result, the external jet potential core extends to less than one diameter in this particular geometrical configuration. For the value of M which was chosen for these experiments, the inner mixing layers merge on the jet-axis at a distance of about 1.5 D_i from the nozzle

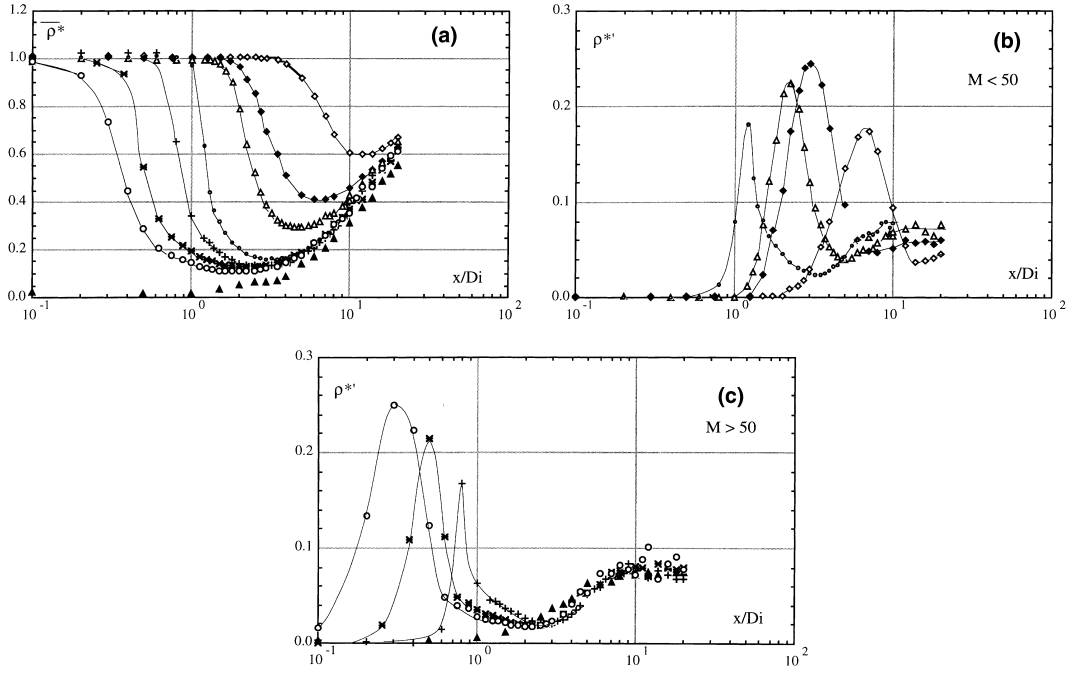

Fig. 8. Influence of the specific momentum flux ratio M on the centreline variations of density. $S = 0.138$; (a) mean density; (b) RMS fluctuations, $M < 50$; $M = (\diamondsuit)$ 1, $(\blacklozenge)$ 4, $(\triangle)$ 9, $(\bigcirc)$ 36; (c) $M > 50$; $(+)$ 64, $(\times)$ 100, $(\bigcirc)$ 144, $(\blacktriangle)$ ∞.

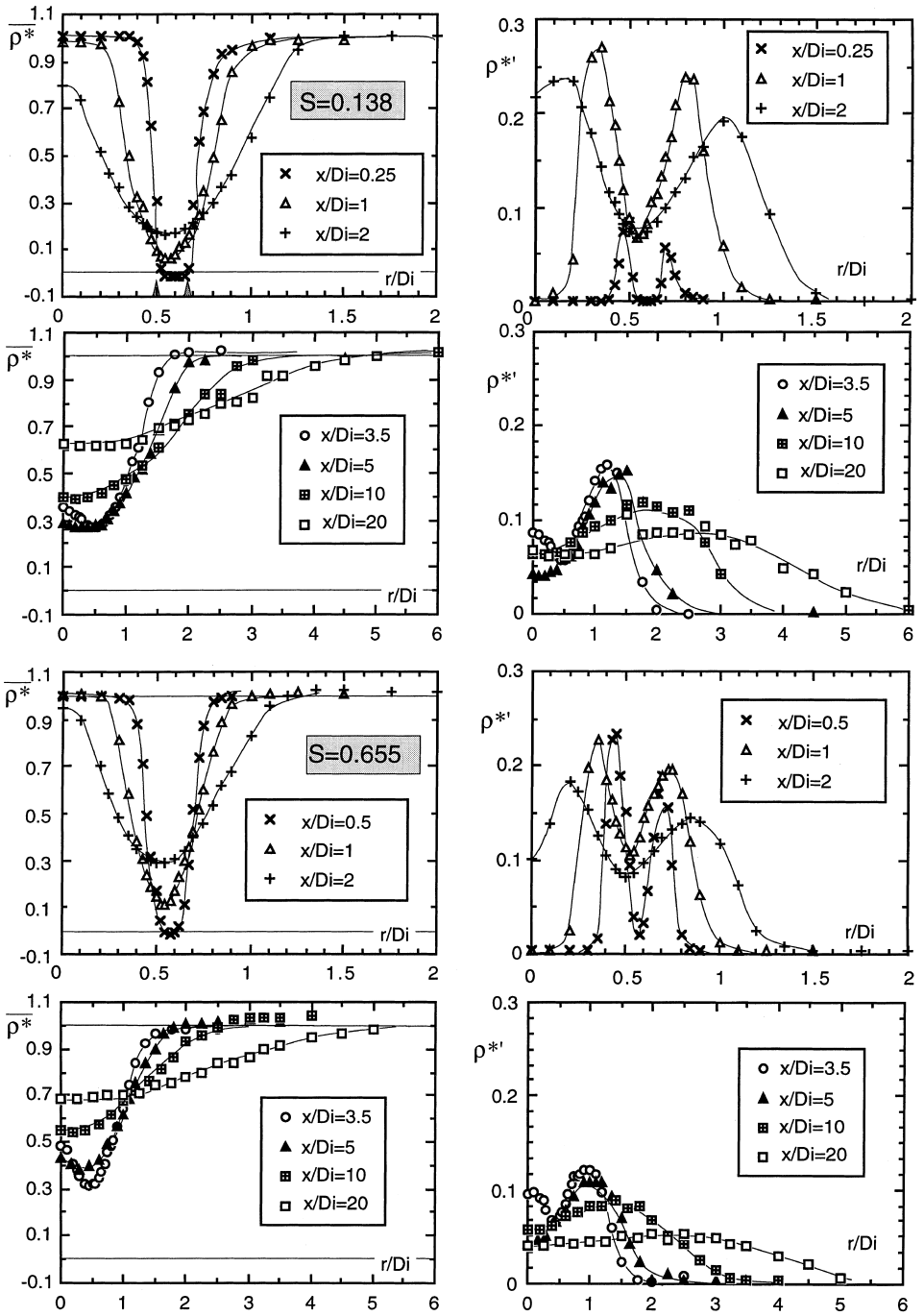

Fig. 9. Mean and RMS density cross-sectional profiles. $M = 9$. Top: $S = 0.138$, $r_v = 8$, $Re_M = 2590$; bottom: $S = 0.655$, $r_v = 3.67$, $Re_M = 5900$.

(Fig. 8(a)). Beyond this distance, $\overline{\rho^*}$ decreases in the downstream direction in the central jet whereas it is still increasing in the coannular jet so that the central region progressively becomes homogeneous. As far as the mean flow is concerned, the mixing process is completed in the central region at $x/D_i \approx 4$–5 for $M = 9$ (see Fig. 9). Farther downstream, the mean and RMS profiles evolve toward the shapes of the round jet. A small influence of S may be observed on Fig. 9 which shows a slower mixing process for the case of moderate density ratio.

For example, the difference between the minimum and the jet-axis values of $\overline{\rho^*}$ is significantly larger for $S = 0.655$ than in the other case at $x/D_i = 3.5$. In addition, the normalised fluctuation level $\rho^{*\prime}$ is systematically lower for $S = 0.655$. This may be an effect of r_v, which is much smaller for this latter case than for the former one.

Results on the mixing layer growth are summarised in Fig. 10(a) which displays the position $r_{0.9}/D_i$ of the points where $\overline{\rho^*} = 0.9$ in the two experiments. These points correspond to the low-speed sides of the external jet mixing layers. The estimated spatial resolution of the probe is reported in the same figure. Very near the nozzle, the high value of $r_{0.9}/D_i$ reached on the outer side of the external jet for $S = 0.138$ may be attributed partly to integration effects of the probe. It has been verified that the mixing layer boundaries as defined by $r_{0.9}/D_i$ are close to those observed in visualisations when the external jet is seeded with smoke. Fig. 10(a) thereby shows a comparison with the results on the visual mixing layer width δ_{vis} obtained by Brown and Roshko [22] in the variable density plane mixing layer. These authors have considered two plane streams with velocities U_1 and U_2 and densities ρ_1 and ρ_2, respectively. They have shown that δ_{vis} is related to the velocity ratio by

$$\frac{d\delta_{vis}}{dx} = C\frac{U_1 - U_2}{U_1 + U_2}, \tag{7}$$

where C is a function of the density ratio. Brown and Roshko found $C = 0.51, 0.38, 0.28$ for $\rho_2/\rho_1 = 7, 1, 1/7$, respectively. For the present experiment, the mixing layer boundaries were computed according to Eq. (7) both for the outer side ($U_1/U_2 = \infty$) and for the inner side ($U_1/U_2 = r_v$) of the external jet and for the two values of S. It was assumed that the mixing layer boundaries were symmetrical with respect to the x-direction for the outer side and for the inner side of the external jet, respectively. According to this computation, for a given value of S, the low-speed side mixing layer boundaries are two straight lines with slopes equal to

$$m_1 = \frac{1}{2}\frac{d\delta_{vis}}{dx} \quad (U_1/U_2 = \infty),$$

$$m_2 = -\frac{1}{2}\frac{d\delta_{vis}}{dx} \quad (U_1/U_2 = r_v),$$

respectively, as given by Eq. (7) (Fig. 10(b)).

On the outer side of the annular jet, the mixing layer growth is in good agreement with the observations of Brown and Roshko. In particular, the enhancement of diffusion for low values of S is also found in the present experiment. The observed slopes are, however, significantly larger on the inner side than on the outer side, whereas the predicted slopes have opposite trends: according to [22], they should decrease by 20% between $U_1/U_2 = \infty$ which corresponds to the outer side and $U_1/U_2 = r_v = 8$ which corresponds to the inner side. This discrepancy may be probably attributed to confinement in the inner potential core and to the resulting adverse pressure gradient.

4.3. Length of the potential core

It is very important to know the length L of the potential core for optimizing the operation of rocket-engines. Fig. 11 summarises results obtained by various techniques in homogeneous coaxial jets [23]. L was determined by laser-anemometry (position of the minimum velocity on the jet-axis) and by laser-sheet visualisations. Complementary results were obtained by using a hot/cold wire probe, consisting of a cold wire placed very close upstream from a hot-wire (typical distance: 20 μm). With this method, L was determined by detecting the RMS fluctuations maximum of the signal given by the cold wire (for more details, see [14]). All of these methods are in remarkable agreement and show that L follows a $M^{-1/2}$ power-law. This result is

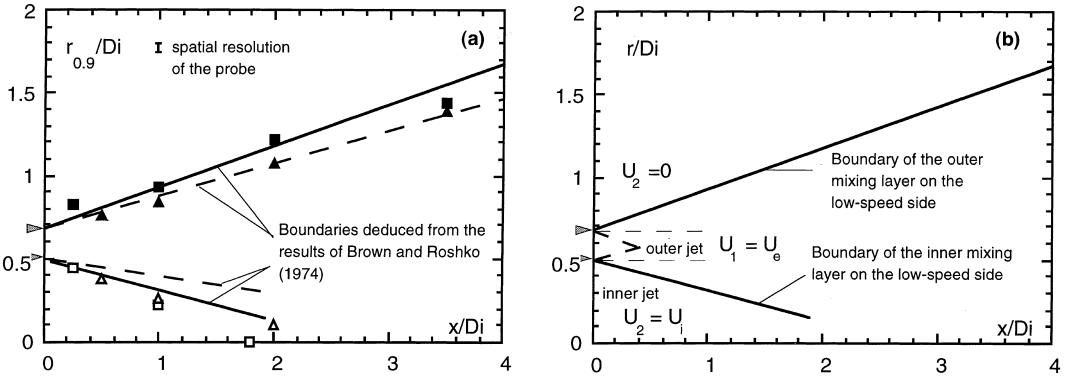

Fig. 10. Mixing layers growth. (a) experimental results; $M = 9$, $S = 0.138$, (■) r_{out}/D_i, (□) r_{int}/D_i; $S = 0.655$, (▲) r_{out}/D_i, (△) r_{int}/D_i. Boundaries of the external jet mixing layers on the low-speed side deduced from Brown and Roshko results: – $S = 0.138$, – – – $S = 0.655$; (b) schematic representation of the mixing layers boundaries.

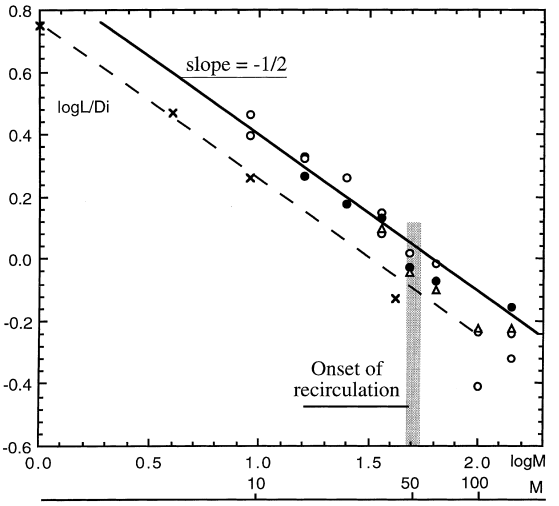

Fig. 11. Length of the potential core. Homogeneous flow: (●) "wake" hot/cold wire probe, (○) laser-sheet visualisations, (△) laser doppler anemometry; $S = 0.655$, (×) aspirating probe.

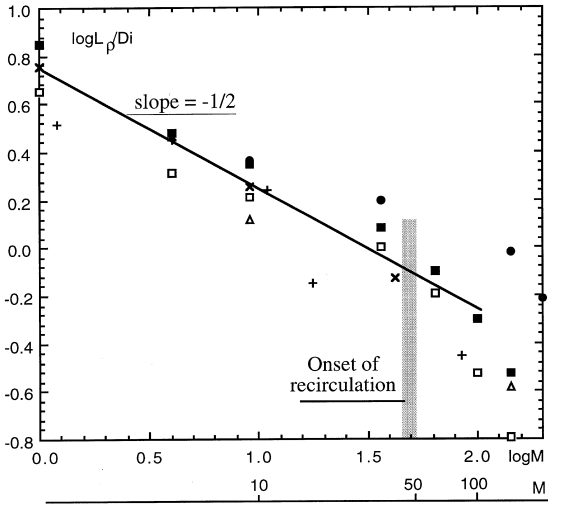

Fig. 12. Influence of the density ratio on the length of the potential core. (×) $S = 0.655$ ambient air, (□) $S = 0.138$ ambient air, (△) $S = 0.138$ ambient helium, (●) $S = 0.028$ ambient helium, (+) Chigier and Beer [12].

also in agreement with the predictions of the model of Rehab et al. [11], who calculated the length of the potential core by equating the mass flow rate issuing from the central nozzle and that entrained across the surface of the potential core. Moreover, the present results compare well with those of Rehab et al. [11] obtained in a geometrically similar water channel. The potential core length was also determined from the density measurements, defining L_p as the distance where $\overline{\rho^*}$ departs from one by a given percentage (say 5%). For the moderate value of S (0.655), the behaviour of L_ρ is quite similar to that of L. L_ρ is, however, smaller than the other determinations of L.

Further measurements carried out for different values of S show that L_p is not considerably affected by density effects when plotted vs M (Fig. 12). Small effects of the density ratio may, however, be observed on Fig. 12, especially for moderate values of M ($M \leqslant 4$). For these latter conditions, L_p is reduced when S is decreased ($S = 0.138$), indicating enhanced entrainment of inner fluid and mixing. This effect seems to disappear for high values of M ($\geqslant 9$), that is to say when the jet dynamics are dominated by pressure gradient effects. It is, however, still observed, when the ambient and the outer jet fluids are the same (helium in this experiment, the inner gas being pure air) in a test conducted at $M = 9$. The centreline $\overline{\rho^*}$ distribution is shown on Fig. 5(d) for these conditions. In this case, it is expected that the external jet is slowed down less rapidly by the ambient fluid, resulting in an increase of entrainment of the central jet by the external jet inner mixing layer. Fig. 12 also displays L_p deduced from the measurements of Chigier and Beer [12]. Although the outer/inner nozzle surface ratio is much larger in this experiment (8.5 instead of 0.82 in the present study), these authors results are in rather good agreement with the present ones.

Some complementary measurements were carried out with a combination of sulfur hexafluoride (SF_6) and helium to feed the inner/outer jets, respectively. The ambient gas was also helium in order to have only two components in the mixture and to enable density measurements with a single aspirating probe. The nozzle was in the downward direction for these experiments. This set of measurements was limited for obvious reasons of cost. The behaviour of these helium/SF_6 coaxial jets with a very low density ratio ($S = 0.028$) seems paradoxical, since when compared to the results obtained for $S = 0.655$, the potential core length is slightly increased for this gas combination (Fig. 12). The same result was deduced from visualisations [14]. Further results may be found in [19]. Contrary to the tendency toward increased mixing observed with a reduction of S, entrainment is then reduced by such further decrease of S and this surprising result has not been explained yet. The mixing process for these helium/SF_6 coaxial jets seems to follow a different behaviour than for the other combinations of gas. Further insight into this phenomenon could be perhaps provided by studying a simpler flow than a coaxial jet, such as, for example, the plane mixing layer.

5. Conclusions

The present study shows that the new aspirating probe is well suited for mean and fluctuating density measurements in variable density jets, except perhaps in

thin layers very close to the nozzle. Density fluctuations are expected to be measured with this probe at frequencies as high as about 1000 Hz. The present results on the density field in coaxial jets with large density differences are in keeping with previous findings obtained by other experimental techniques [14]. The density field is strongly affected by the dynamics of the flow; however, the present measurements show that density effects on mixing are rather well taken into account by considering the outer to inner jet flux momentum ratio M, instead of the velocity ratio r_v and the density ratio S separately. This observation confirms the important role played by M in the dynamics of variable density coaxial jets.

The length of the potential core deduced from density measurements on the jet axis varies as $M^{-1/2}$ for moderate values of S, in agreement with simple calculations. A reduction of this length is observed for density ratios much smaller than one ($S \approx 0.14$) in the low-M range. This effect is consistent with the behaviour of the mixing layer with density differences. The opposite behaviour occurs for extremely low values of S and this unexpected result has not been explained yet. Further investigations in a simpler configuration such that of a plane mixing layer would be worth of interest for these low values of S.

Acknowledgements

This research was partially supported by the Société Européenne de Propulsion. The authors would like to gratefully acknowledge The National Council of Technological and Scientific Development of Brazil for supporting the stay of E.B. Camano Schettini in LEGI.

References

[1] F.H. Champagne, I.J. Wygnanski, An experimental investigation of coaxial jets, Int. J. Heat Mass Transfer 14 (1971) 1445–1461.
[2] N.W.M. Ko, A.S.H. Kwan, The initial region of subsonic coaxial jets, J. Fluid Mech. 73 (2) (1976) 305–332.
[3] A.S.H. Kwan, N.W.M. Ko, Coherent structures in subsonic coaxial jets, J. Sound Vib. 48 (2) (1976) 203–219.
[4] A.S.H. Kwan, N.W.M. Ko, Covariance measurements in the initial region of coaxial jets, J. Sound Vib. 52 (4) (1977) 567–578.
[5] N.W.M. Ko, H. Au, Coaxial jets of different mean velocity ratios, J. Sound Vib. 100 (2) (1985) 211–232.
[6] H. Au, N.W.M. Ko, Coaxial jets of different mean velocity ratios, part 2, J. Sound Vib. 116 (3) (1987) 427–443.
[7] W.J.A. Dahm, C.E. Frieler, G. Tryggvason, Vortex structure and dynamics in the near field of a coaxial jet, J. Fluid Mech. 241 (1992) 371–402.
[8] N.W.M. Ko, W.T. Chan, The initial region of annular jets, J. Fluid Mech. 93 (1979) 549–584.
[9] E.B. Camano, M. Favre-Marinet, On the initial region of inhomogeneous coaxial jets, in: R. Benzi (Ed.), Advances in Turbulence V, Kluwer Academic Publishers, Dordrecht, 1994, pp. 58–62.
[10] E. Villermaux, H. Rehab, E.J. Hopfinger, Breakup regimes and self-sustained pulsations in coaxial jets, Meccanica 29 (4) (1994) 393–401.
[11] H. Rehab, E. Villermaux, E.J. Hopfinger, Flow regimes of large velocity ratio coaxial jets, J. Fluid Mech. 345 (1997) 357–381.
[12] N.A. Chigier, J.M. Beer, The flow region near the nozzle in double concentric jets, J. Basic Eng., Trans. ASME, Series D 86 (4) (1964) 797–804.
[13] P. Gladnick, J. Enotiadis, J. LaRue, G. Samuelsen, Near-field characteristics of a turbulent coflowing jet, AIAA J. 28 (8) (1990) 1405–1414.
[14] M. Favre-Marinet, E. Camano, J. Sarboch, Near-field of coaxial jets with large density differences, Exp. Fluids 26 (1999) 97–106.
[15] T.S. Zawacki, H. Weinstein, Experimental investigation of turbulence in the mixing region between coaxial streams, NASA CR. 959 Washington, 1968.
[16] G.L. Brown, M.R. Rebollo, A small fast-response probe to measure composition of a binary mixture, AIAA J. 10 (5) (1972) 649–652.
[17] S.A. Ahmed, R.M.C. So, Concentration distributions in a model combustor, Exp. Fluids 4 (1986) 107–113.
[18] R. Riva, Ecoulements de fluides inhomogènes :stabilité des jets, transferts turbulents dans les couches limites. Thèse INP, Grenoble, 1991.
[19] E.B. Camano, Etude expérimentale des jets coaxiaux avec différences de densité. Thèse INP, Grenoble, 1996.
[20] W.M. Pitts, Effects of global density ratio on the centerline mixing behavior of axisymmetric turbulent jets, Exp. Fluids 11 (1991) 125–134.
[21] C.J. Chen, W. Rodi, Vertical buoyant jets – a review of experimental data, in: The Science and Application of Heat and Mass Transfer, Pergamon Press, New York, 1980.
[22] G.L. Brown, A. Roshko, On density effects and large structure in turbulent mixing layers, J. Fluid Mech. 64 (4) (1974) 775–816.
[23] M. Favre-Marinet, E. Camano, J. Sarboch, Mixing in coaxial jets with large density differences, in: Proceedings of the 11th Turbulent Shear Flows Conference, Grenoble, 1997.